

Properties of the quaternary half-metal-type Heusler alloy

$\text{Co}_2\text{Mn}_{1-x}\text{Fe}_x\text{Si}$.

Benjamin Balke, Gerhard H. Fecher, Hem C. Kandpal, and Claudia Felser*

*Institut für Anorganische und Analytische Chemie,
Johannes Gutenberg - Universität, D-55099 Mainz, Germany.*

(Dated: December 2, 2024)

Abstract

This work reports on the bulk properties of the quaternary Heusler alloy $\text{Co}_2\text{Mn}_{1-x}\text{Fe}_x\text{Si}$ with the Fe concentration ranging from $x = 0$ to 1 in steps of 0.1. All samples, which were prepared by arc melting, exhibit $L2_1$ long range order over the complete range of Fe concentration. Structural and magnetic properties of $\text{Co}_2\text{Mn}_{1-x}\text{Fe}_x\text{Si}$ Heusler alloys were investigated by means of X-ray diffraction, high and low temperature magnetometry, Mössbauer spectroscopy and differential scanning calorimetry. The magnetization of the Fe doped Heusler alloys is in agreement with the values of the magnetic moments expected for a Slater-Pauling like behavior of half-metallic ferromagnets. The experimental findings are discussed on the hand of self-consistent calculations of the electronic and magnetic structure. To achieve good agreement with experiment, the calculations indicate that on-site electron-electron correlation must be taken into account, even at low Fe concentration.

PACS numbers: 75.30.-m, 71.20.Be, 61.18.Fs

Keywords: half-metallic ferromagnets, electronic structure, magnetic properties, Heusler compounds

*Electronic address: fecher@uni-mainz.de

I. INTRODUCTION

Kübler *et al* [1] recognized that the minority-spin state densities at the Fermi energy nearly vanish for Co_2MnAl and Co_2MnSn . The authors concluded that this should lead to peculiar transport properties in these Heusler compounds because only the majority density contributes. The so called half-metallic ferromagnets have been proposed as ideal candidates for spin injection devices because they have been predicted to exhibit 100 % spin polarization at the Fermi energy (ϵ_F) [2]. From the applications point of view, a high Curie temperature for a half-metallic ferromagnet may be an important condition. For this reason, Heusler alloys with $L2_1$ structure have attracted great interest. Some of these alloys exhibit high Curie temperatures and, according to theory, should have a high spin polarization at the Fermi energy [3, 4, 5]. Calculations also show that anti-site disorder will destroy the high spin polarization [6], implying that precise control of the atomic structure of the Heusler alloys is required.

The Heusler alloy Co_2MnSi has attracted particular interest because it is predicted to have a large minority spin band gap of 0.4 eV and, at 985 K, has one of the highest Curie temperature, among the known Heusler compounds [7, 8]. Structural and magnetic properties of Co_2MnSi have been reported for films and single crystals [9, 10, 11, 12, 13, 14]. In accordance with theoretical predictions, bulk Co_2MnSi has been stabilized in the $L2_1$ structure with a magnetization of $5 \mu_B$ per formula unit. From tunneling magneto resistance (TMR) data with one electrode consisting of a Co_2MnSi film Schmalhorst *et al* [15, 16] inferred a spin polarization of 61 % at the barrier interface. Although the desired spin polarization of 100 % was not reached, the experimental value of the spin polarization is larger than the maximum 55 % effective spin polarization of a variety of 3d-transition metal alloys in combination with Al_2O_3 barriers [17]. However, the spin polarization of photoelectrons emerging from single crystalline Co_2MnSi films grown on GaAs by pulsed laser deposition indicate a quite low spin polarization at the Fermi level of only 12 % at the free surface [14]. Wang *et al* [13, 14] assumed that partial chemical disorder was responsible for this discrepancy with the theoretical predictions.

Recent investigations [18, 19, 20, 21] of the electronic structure of Heusler compounds indicate that on-site correlation plays an important role in these compounds and may serve to destroy the half-metallic properties of Co_2MnSi . In addition, if on-site correlation is

considered in electronic structure calculations Co_2FeSi becomes a half-metallic ferromagnet with a magnetic moment of $6 \mu_B$. The present investigation focuses on searching for a mixed compound where the half-metallic behavior, and thus the magnetic moment, is stable against the variation of on-site correlation.

II. COMPUTATIONAL DETAILS

The present work reports on calculations of the electronic and magnetic properties of ordered Heusler compounds of the $\text{Co}_2(\text{Mn}_{(1-x)}\text{Fe}_x)\text{Si}$ type. The random alloys were treated as virtual crystals of the $\text{Co}_2\text{Mn}_{(1-i/4)}\text{Fe}_{i/4}\text{Si}$ type with $i = 0, 1, 2, 3, 4$. Non-rational values of x as well as random disorder (for examples see references [22, 23, 24]) will not be discussed here.

The self-consistent electronic structure calculations were carried out using the scalar-relativistic full potential linearized augmented plane wave method (FLAPW) as provided by Wien2k [25]. In the parameterization of Perdew *et al* [26] the exchange-correlation functional was taken within the generalized gradient approximation (GGA). A $20 \times 20 \times 20$ mesh was used for integration of cubic systems, resulting in 255 k -points in the irreducible wedge of the Brillouin zone.

The properties of pure compounds containing Mn or Fe were calculated in $F\ m\bar{3}m$ symmetry using the experimental lattice parameter ($a = 10.658a_{0B}$, $a_{0B} = 0.529177 \text{ \AA}$) determined by X-ray powder diffraction. Co atoms are placed on 8c Wyckoff positions, Mn or Fe on 4a and Si on 4b [40]. All muffin tin radii were set as nearly touching spheres with $r_{MT} = 2.3a_{0B}$. A structural optimization for the pure compounds showed that the calculated lattice parameter deviates from the experimental one only marginally.

The calculation of mixed random alloys is not straight forward in the FLAPW as is used here. However, the substitution of some Mn atoms of the $L2_1$ structure by Fe leads in certain cases to ordered structures that can be easily used for the calculations. Those ordered, mixed compounds have the general formula sum $\text{Co}_8(\text{Mn}_{(1-x)}\text{Fe}_x)_4\text{Si}_4$ and have integer occupation of Mn and Fe if $x = i/4$ where $i = 1, 2, 3$. (for more details see Ref.[24]). To verify that ordered compounds could be used instead of random alloys, the full relativistic Korringa-Kohn-Rostocker (KKR) method with the coherent potential approximation (CPA) was employed [27]. The exchange-correlation functional was parameterized by using the plain

GGA. No significant differences in the integrated properties, such as the density of states or the magnetic moments, were found between the methods.

For the case of Co_2FeSi , it has recently been demonstrated that LSDA or GGA schemes are not sufficient for describing the electronic structure correctly. Significant improvement was found, however, when the LDA+ U method [18, 21] was used and this computational scheme was used here as well. LDA+ U , as described by Anisimov *et al* [28], adds an orbital dependent electron-electron correlation, which is not included in the plain LSDA or GGA schemes. It should be mentioned that the + U was used here with the GGA rather than the LSDA parameterization of the exchange-correlation functional. No significant differences were observed using either of these parameterizations.

III. EXPERIMENTAL DETAILS

$\text{Co}_2\text{Mn}_{1-x}\text{Fe}_x\text{Si}$ samples were prepared by arc melting of stoichiometric amounts of the constituents in an argon atmosphere at 10^{-4} mbar. Care was taken to avoid oxygen contamination. This was ensured by evaporating Ti inside of the vacuum chamber before melting the compound as well as by additional purifying of the process gas. The polycrystalline ingots that were formed were then annealed in an evacuated quartz tube at 1273 K for 21 days. This procedure resulted in samples exhibiting the Heusler type $L2_1$ structure, which was verified by X-ray powder diffraction (XRD) using excitation by Cu K_α or Mo K_α radiation.

Flat disks were cut from the ingots and polished for spectroscopic investigations of bulk samples. For powder investigations, the remainder was crushed by hand using a mortar. It should be noted that using a steel ball mill results in a strong perturbation of the crystalline structure.

X-ray photo emission (ESCA) was used to verify the composition and to check the cleanliness of the samples. After removal of the native oxide from the polished surfaces by Ar^+ ion bombardment, no impurities were detected with ESCA. The samples were afterwards capped in-situ by a 2 nm layer of Au at room temperature to prevent oxidation of the samples during transport in air.

Magneto-structural investigations were carried using Mössbauer spectroscopy in transmission geometry using a constant acceleration spectrometer. For excitation, a $^{57}\text{Co}(\text{Rh})$ source with a line width of 0.105 mm/s was used. The spectra from powder samples were

taken at 290 K.

The magnetic properties were investigated by a super conducting quantum interference device (SQUID, Quantum Design MPMS-XL-5) using nearly punctual pieces of approximately 5 mg to 10 mg of the sample. Differential scanning calorimetry (DSC) measurements (NETZCH, STA 429) were performed to detect phase transitions below the melting point. In particular, attempts were made to find the Curie temperature (T_C), but this turned out to be too high to be determined directly by the SQUID, which is limited to 775 K even in the high temperature mode.

IV. RESULTS AND DISCUSSION

A. Electronic Properties

The electronic structure of the substitutional series $\text{Co}_2\text{Mn}_{(1-i/4)}\text{Fe}_{i/4}\text{Si}$ with $i = 0, \dots, 4$ was calculated using the LDA+ U method. This method was used because it was found that plain GGA calculations are not sufficient to explain the magnetic moments in Co_2FeSi [18]. Using the impurity model of Anisimov and Gunnarsson [29] along with self consistent calculations, the effective Coulomb-exchange parameter U_{eff} was determined for the pure compounds containing Mn and Fe. Details of the procedure and the implementation of the constrained LDA calculations in FLAPW are reported by Madsen and Novak [30]. The values found in the present work are $U_{Co} = 0.30$ Ry and $U_{Mn} = 0.39$ Ry for Co_2MnSi , and $U_{Co} = 0.31$ Ry and $U_{Fe} = 0.32$ Ry for Co_2FeSi .

Comparing the semi-empirical values used in [21] to the values found here from the constrained LDA calculations, it is evident that the latter are too high to explain the magnetic moments. Additional calculations for the elemental 3d transition metals revealed that all values for U_{eff} found in the constrained LDA calculations are considerably too high to explain those metallic systems correctly. This is despite the fact that such calculations may result in reliable values for Mott insulators [31].

For these reasons, the semi-empirical values corresponding to 7.5 % of the atomic values (see: Ref.[21]) will be used and discussed here. These values ensure that the calculated magnetic moments agree with the measured values over the entire range of the Fe concentration (compare Sec.: IV D). In particular, the values for U_{eff} were set to $U_{Co} = 0.14$ Ry,

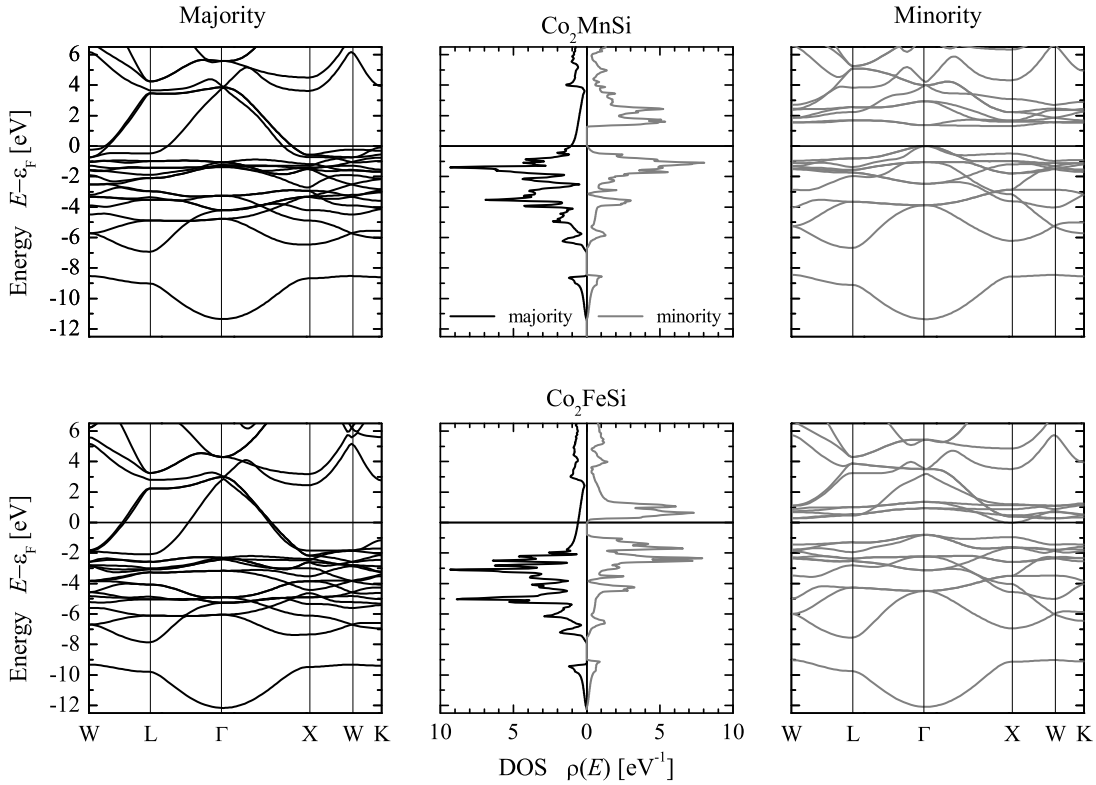


FIG. 1: Band structure and density of states of Co_2MnSi and Co_2FeSi .

$U_{Fe} = 0.132$ Ry, and $U_{Mn} = 0.13$ Ry, independent of the iron concentration. These values are closer to the values for the Coulomb interaction U_{dd} for d electrons in the elemental $3d$ transition metals reported by Bandyopadhyay and Sarma [32] even before the LDA+ U method itself was introduced.

Figure 1 shows the spin resolved band structure and the total density of states for the pure compounds Co_2MnSi and Co_2FeSi as calculated within the framework of the LDA+ U . In all cases, the band structures are very similar and the gap in the minority bands is clearly revealed.

When explaining the Heusler half-metallic ferromagnets using simple rigid band-like or molecular orbital-like models, it is expected that the additional d electron of the Fe compound fills the majority states while not affecting the minority states. As may be seen from Fig.: 1, this is clearly a strong oversimplification. The additional electron must be absorbed in the strongly dispersing unoccupied d -bands seen in the Mn compound just above ϵ_F . Comparing the majority DOS, it can be seen that the high density d -states at -1.4 eV (or

-3.5 eV) in Co_2MnSi are shifted to approximately -3 eV (or -5 eV) in Co_2FeSi . Keeping the minority DOS fixed, this would imply an additional exchange splitting of about 1.6 eV, when compared to Co_2MnSi , between the majority and minority states in Co_2FeSi . This large and rather unphysical shift indicates that the rigid band model fails and that other alterations of the band structure must take place.

After inspecting the electronic structure in more detail, some particular changes are found. For example, the rather large shift of the occupied majority d -states is compensated by a shift of the occupied minority d -states, and this keeps the exchange splitting rather fixed. This then results in a shift and splitting of the occupied minority d -states (seen at -1 eV in the Mn compound and at -1.7 eV or -2.3 eV in the Fe compound) as well as a shift of the unoccupied minority d -states towards the Fermi energy. In addition, the splitting of the unoccupied minority d -states just above the gap is reduced from 0.7 eV in Co_2MnSi to 0.4 eV in Co_2FeSi . The most striking effect, however, is the shift of the Fermi energy from the top of the minority valence band to the bottom of the minority conduction band. These particular positions of the minority gap with respect to the Fermi energy make both systems rather unstable with respect to their electronic and magnetic properties. Any small change of a physically relevant quantity may serve to destroy the HMF character by shifting the Fermi energy completely outside of the minority gap. As long as the shift is assumed to be small, the magnetic moment may still be similar to the one expected from a Slater-Pauling behavior, even so, the minority gap is destroyed. For this reason, the magnetic moment may not provide evidence for a half-metallic state.

It is to be immediately expected that the situation improves in the mixed compounds containing both Mn and Fe. Figure 2 shows the spin resolved total density of states for the compounds with an intermediate Fe concentration ($x \neq 0, 1$). In all cases, the gap in the minority bands is kept.

The shift of the majority d -states with low dispersion away from the Fermi energy is clearly visible in Fig: 2. The additional charge (with increasing Fe concentration x) is filling the strongly dispersing d -states in the majority channel. At the same time, the minority DOS is shifted with respect to the Fermi energy such that ϵ_F moves from the top of the minority valence bands at low x to the bottom of the minority conduction bands at high x . In general, it can be concluded that the additional electrons affect both majority and minority states. For intermediate Fe concentrations, the Fermi-energy falls in the middle of

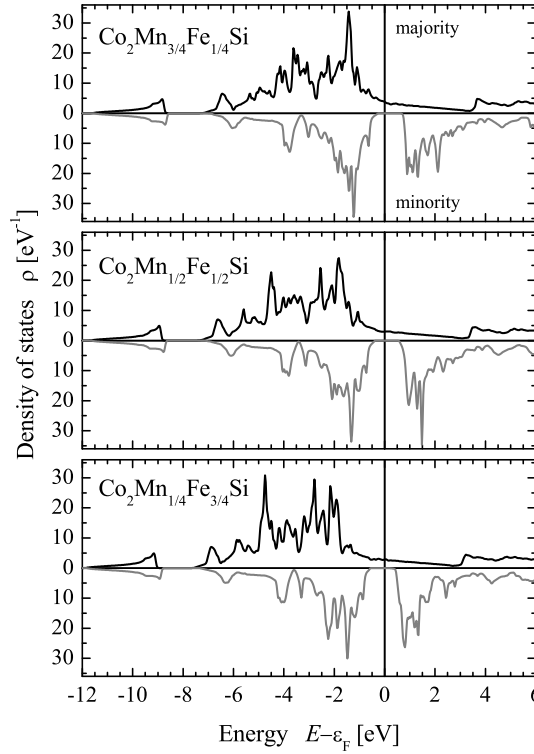


FIG. 2: Spin resolved density of states of $\text{Co}_2\text{Mn}_{1-x}\text{Fe}_x\text{Si}$ for $x = 1/4, 1/2$, and $3/4$.

the gap in the minority states. This situation makes the magnetic and electronic properties of the compound very stable against external influences that will not be able to change the number of minority electrons. This applies both to the parameters in the theoretical calculations as well as the actual experimental situation.

If the Heusler alloys are half-metallic ferromagnets, then they will show a Slater-Pauling behavior for the magnetization, meaning that the saturation magnetization scales with the number of valence electrons [3, 5, 33]. The magnetic moment per unit cell (in multiples of the Bohr magneton μ_B) is given by:

$$m = N_V - 24, \quad (1)$$

with N_V denoting the accumulated number of valence electrons in the unit cell. For Co_2MnSi there is a total of $2 \times 9 + 7 + 4 = 29$ valence electrons in the unit cell and accordingly 30 for Co_2FeSi . for this reason the magnetic moment is expected to vary linearly from $5 \mu_B$ to $6 \mu_B$ with increasing iron concentration in $\text{Co}_2\text{Mn}_{1-x}\text{Fe}_x\text{Si}$.

TABLE I: Total magnetic moments of ordered $\text{Co}_2\text{Mn}_{1-x}\text{Fe}_x\text{Si}$.

All moments were calculated for the given super-cells. Their values are in μ_B and respect 4 atoms in the unit cell for easier comparison.

compound	x	GGA	LDA+ U
Co_2MnSi	0	5.00	5.00
$\text{Co}_8\text{Mn}_3\text{FeSi}_4$	1/4	5.21	5.25
$\text{Co}_4\text{MnFeSi}_2$	1/2	5.44	5.50
$\text{Co}_8\text{MnFe}_3\text{Si}_4$	3/4	5.55	5.75
Co_2FeSi	1	5.56	6.00

The results found from the LDA+ U calculations for the magnetic moments are summarized in Tab.: I and compared to pure GGA calculations without the inclusion of the U type correlation. It is evident from Tab.: I that the GGA derived values do not follow the Slater-Pauling curve (with the exception of Co_2MnSi), whereas the values from the LDA+ U follow the curve closely. These results again indicate the loss of the minority gap - and thus the loss of half-metallicity - if the on-site correlation is not included.

B. Structural Properties

Structural characterization has been performed with X-ray diffraction (XRD) of powders as the standard method. Due to the small differences in the scattering factors between the $3d$ metals Mn, Fe and Co, structural information, other than a simple confirmation of a single cubic phase can only be gained by measuring the comparatively small (5 % of the (220)-peak) (111) and (200) superstructure peaks that are typical for the face centered cubic (fcc) lattice. The simulated powder diffraction pattern of Co_2MnSi shows the decisive (111) and (200) peaks for the defect-free structure. Both of these super-lattice peaks vanish for a random occupation of all lattice sites (4a, 4b, and 8c) resulting in the $A2$ structure. In the case of random occupation of 4a and 4b sites by Mn, Fe, and Si, only the (200) super-lattice peak of the $B2$ structure type would be seen, while the (111) peak would vanish.

Such types of disorder would close the gap in the minority DOS so that the material would no longer be a half-metallic ferromagnet [20, 24]. However, the magnetic moments

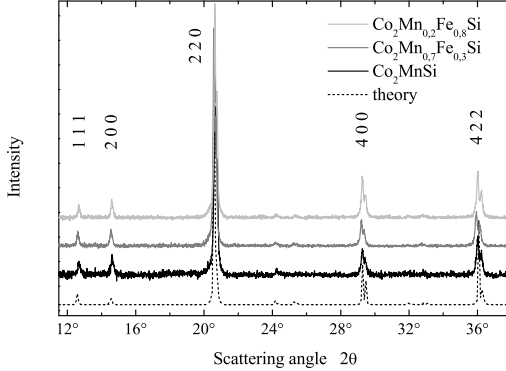


FIG. 3: XRD spectra for Co_2MnSi and $\text{Co}_2\text{Mn}_{0.8}\text{Fe}_{0.2}\text{Si}$.

The spectra were excited by Mo K_α radiation.

may still follow a Slater-Pauling like behavior. The half-metallic character is also destroyed when only one of the Co atoms is exchanged by Mn/Fe (X structure [34] with symmetry $F\bar{4}3m$). This type of disorder shows up as a (111) super-lattice peak with higher intensity than the (200) peak.

As expected for the defect-free structure, the experimental data show both the (111) and (200) peaks with equal intensity for all Fe concentrations indicating the presence of a long range fcc structure for all samples (see Fig.: 3). Within the uncertainty of the experiment, the lattice parameter of 5.64 \AA remains nearly independent of the Fe concentration .

Because the scattering factors of all three transition metals are very similar, X-ray diffraction cannot easily discern a disorder when the Mn and Fe are partially exchanged with Co atoms on both 8a positions (DO_3 like disorder). Because both have the same $F\bar{m}\bar{3}m$ symmetry, this leads to nearly identical diffraction patterns when going from the $L2_1$ to the DO_3 structure. As will be shown in the next section, this type of disorder can be ruled out by means of Mössbauer spectroscopy.

C. Magneto-structural Properties

^{57}Fe Mössbauer spectroscopy was performed to investigate the magneto-structural properties. The transmission spectrum of $\text{Co}_2\text{Mn}_{0.5}\text{Fe}_{0.5}\text{Si}$ is shown in Fig.: 4. Starting from 10 %, the spectra for the complete range of Fe concentration x are all similar and therefore not shown here. The observed sextet-like pattern is typical for a magnetically ordered sys-

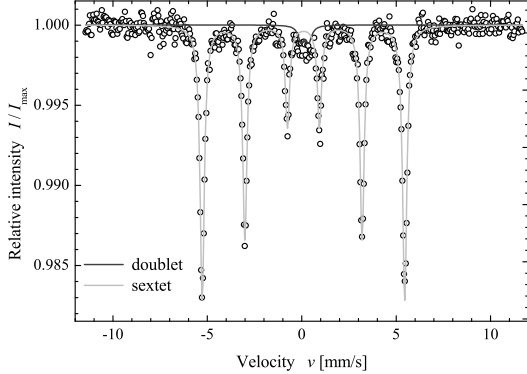


FIG. 4: ^{57}Fe Mössbauer spectrum of $\text{Co}_2\text{Mn}_{0.5}\text{Fe}_{0.5}\text{Si}$.

The spectrum was taken at 290K and excited by a $^{57}\text{Co}(\text{Rh})$ source. Solid lines are results of a fit to determine the sextet and doublet contributions and to evaluate the hyperfine field.

tem. The pattern is typical for the cubic symmetry and no asymmetric shift of the lines from a non-cubic quadrupole interaction is observed.

The spectrum shown in Fig.: 4 for 50 % Fe is dominated by an intense sextet. With Fe occupying the 4a sites with cubic symmetry (O_h), this sextet indicates on the high order of the sample. In addition to the sextet, a much weaker line at the center of the spectrum is visible. Depending upon the composition it can be explained as a singlet or doublet. Its contribution to the overall intensity of the spectrum is approximately 3.5 % at $x = 0.5$. The origin of the singlet or doublet may be caused by anti-site disorder leading to a small fraction of paramagnetic Fe atoms. The splitting of the paramagnetic line into a doublet is due to dynamic effects and, among others reasons, usually depends upon the size of the powder grains. The slight disorder arises most likely from surface regions of the sample that are destroyed when the sample is crushed to powder. A partial contamination of the relatively large surface area of the powder with oxygen can also not been excluded. The relative contribution of the doublet decreases exponentially from 9 % in low Fe-substituted $\text{Co}_2\text{Mn}_{0.9}\text{Fe}_{0.1}\text{Si}$ to 1.8 % in pure Co_2FeSi . As was also suggested by the photo absorption and ESCA measurements, this may indicate a larger probability for oxidation in the Mn rich part of the series.

The line width of the sextet is approximately (0.14 ± 0.01) mm/s on average over the complete series of compositions. A pronouncedly higher line width of $\approx 0.19\text{mm/s}$ was found for the alloy with $x = 0.7$. This indicates a higher disorder in that sample and may also

explain the slightly higher magnetic moment (compare Fig.: 8 in Sec.: IV D). The isomer shift increases linearly from 0.075 mm/s to 0.129 mm/s with increasing x , indicating the change in the environment of the Fe atoms, that appears here in the second nearest neighbor shell where the next Fe or Mn atoms are located. Despite this increase, the values suggest a Fe^{3+} -like character of the iron atoms in $\text{Co}_2\text{Mn}_{1-x}\text{Fe}_x\text{Si}$.

The hyperfine field (HFF) at the Fe sites amounts to 26.5×10^6 A/m in $\text{Co}_2\text{Mn}_{0.5}\text{Fe}_{0.5}\text{Si}$. This is the maximum value observed in the complete series with varying Fe concentration x . Overall, the hyperfine field varies nonlinearly from 25.9×10^6 A/m at $x = 0.1$ to 25×10^6 A/m at $x = 1$ (see also: [41]). It should be noted that the Mössbauer spectra taken at 85K from Co_2FeSi exhibited a considerably higher value (26.3×10^6 A/m) without additional singlet or doublet contributions. Therefore, thermally activated fluctuations or disorder can not be excluded here. The values of the HFF at the Fe atoms are comparable to those found by Niculescu *et al* [35, 36] using spin-echo nuclear magnetic resonance (NMR). For $\text{Co}_{3-x}\text{Fe}_x\text{Si}$, these authors reported approximately 26.9×10^6 A/m for 4a sites. The values for partial occupancy of 8c sites, expected from NMR [36] ($\approx 16 \times 10^6$ A/m) for Co_2FeSi are considerably smaller. This is in agreement with calculations for Co and Fe on interchanged sites ($\approx 17 \times 10^6$ A/m). Therefore, a DO_3 type disorder can be excluded. The calculated hyperfine fields are, however, nearly independent of the Fe concentration. They decrease linearly with x by -0.7×10^6 A/m from 27.01×10^6 A/m for Co_2FeSi . A maximum in the $H_{HFF}(x)$ dependence at $x = 1/2$ could not be verified. It was found neither for the ordered compounds using the FLAPW method with the LDA+ U , nor for random alloys calculated using a KKR-CPA scheme in the GGA approximation.

Differential scanning calorimetry was used to find the high temperature phase transitions in the substitutional series. Figure 5 shows a typical result from DSC, which was used to investigate the expected phase transitions. The figure displays the change of the DSC signal as a function of the temperature using nominal heating and cooling rates of 20 K/min. A strong signal arising from a phase transition is easily detected at about 1000 K to 1050 K during both heating and cooling. The shift of the maxima is mainly due to an intrinsic hysteresis effect of the methods and depends on the temperature rates and the actual amount of material. The length of the error bars in Fig.: 6 corresponds to this hysteresis.

A series of DSC measurements was performed with different scanning rates for heating and cooling, but it was not possible to distinguish the magnetic transition temperature

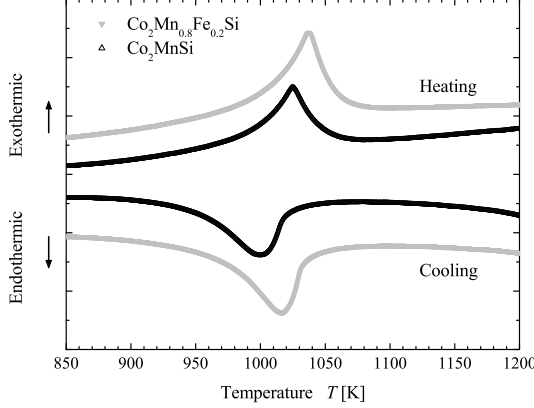


FIG. 5: DSC results for Co_2MnSi and $\text{Co}_2\text{Mn}_{0.8}\text{Fe}_{0.2}\text{Si}$.

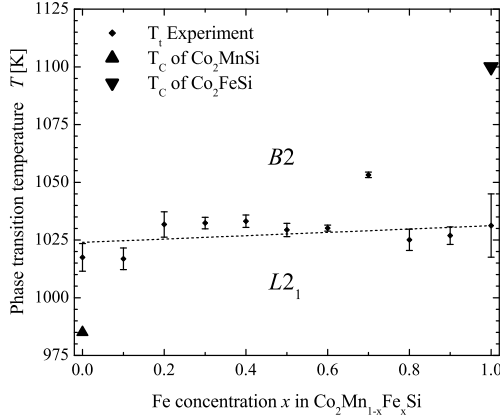


FIG. 6: Phase transitions in $\text{Co}_2\text{Mn}_{1-x}\text{Fe}_x\text{Si}$.

The straight line is the result of a linear fit of $T_t(x)$ as function of the Fe concentration. The given Curie temperatures are taken from Refs. [38] and [18] for Co_2MnSi and Co_2FeSi , respectively.

because it was too close to the structural transition temperature of the $L2_1$ to the $B2$ phase $T_t^{B2 \leftrightarrow L2_1}$. To overcome the problem of nearby phase transitions of different kind, it would be necessary to obtain high temperature magnetization curves such as those that Kobayashi et al. [37] obtained in their examination of the series $\text{Co}_2\text{Cr}_{1-x}\text{Fe}_x\text{Ga}$, or the difference in the transition temperatures should be more than 100 K.

Figure 6 displays the temperature dependence of the $L2_1 \leftrightarrow B2$ phase transition. It is nearly constant, increasing slightly, as the Fe content increases, from ≈ 1024 K for Co_2MnSi to ≈ 1031 K for Co_2FeSi . It is seen that the Curie temperatures of the end members of the substitutional series are slightly below or above the structural phase transition for the

compound containing Mn or Fe, respectively. The Curie temperature is expected to increase with increasing x from $T_C(0) = 985$ K [38] to $T_C(1) = 1100$ K [18], while in $\text{Co}_2\text{Mn}_{1-x}\text{Fe}_x\text{Si}$ $T_t^{B2 \leftrightarrow L2_1}$ hardly varies with increasing x , being around 1027 K for $x = 0.5$. It is therefore impossible here to unambiguously determine T_C by using the DSC technique, because of the relative weakness of the magnetic transition compared to the structural transition and the overlap of those two transitions in the DSC spectra. It is interesting to note that the Curie temperature of the compounds with high Fe concentration appears to be above the order-disorder phase transition.

D. Magnetic Properties

The Co_2 -based Heusler alloys that are half-metallic ferromagnets show a Slater-Pauling like behavior for the magnetization (see Sec.: IV A). The saturation magnetization scales with the number of valence electrons [5] and the magnetic moment per unit cell is given by Eq.: 1. A magnetic moment of:

$$m(x) = (5 + x)\mu_B \quad (2)$$

is expected for $\text{Co}_2\text{Mn}_{1-x}\text{Fe}_x\text{Si}$.

Low temperature magnetometry was performed by means of the SQUID to check the calculated saturation moment. Selected results are shown in Fig.: 7. The increase of the saturation moment with the iron concentration is clearly visible. In addition, it is found that all $\text{Co}_2\text{Mn}_{1-x}\text{Fe}_x\text{Si}$ samples are soft magnetic with a small remanence and a small coercive field. Results for the element-specific magnetic moments from X-ray magnetic circular dichroism are reported elsewhere [39].

The total magnetic moments, measured at 5 K and in saturation, are $(4.97 \pm 0.05)\mu_B$ and $(5.97 \pm 0.05)\mu_B$ for the pure compounds Co_2MnSi and Co_2FeSi , respectively. The latter is in perfect agreement with the recent investigation reported in Refs.[18, 19]. Figure 8 displays the dependence of the saturation moment as a function of the Fe concentration x . The series shows a nearly linear increase of m with increasing Fe concentration that closely fits the values expected from a Slater-Pauling like behavior.

Comparing the experimental results to the theoretical values as given in Tab.: I, it is evident that they closely agree with those from the LDA+ U calculations. The agreement

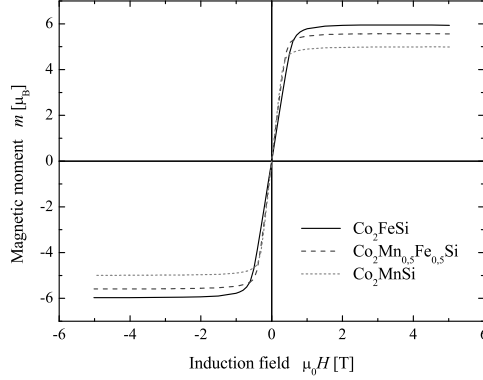


FIG. 7: Magnetization of $\text{Co}_2\text{Mn}_{1-x}\text{Fe}_x\text{Si}$.

Displayed are the hysteresis curves for $x = 0, 0.5, 1$ taken at $T = 5$ K.

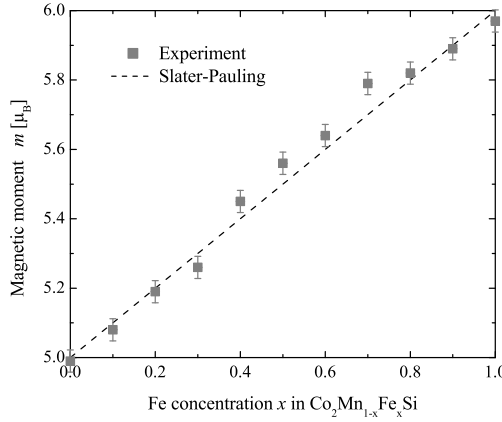


FIG. 8: Concentration dependence of the magnetic moment in $\text{Co}_2\text{Mn}_{1-x}\text{Fe}_x\text{Si}$.

All measurements were performed at $T = 5$ K.

of the GGA result for Co_2MnSi may thus be seen as due to chance. The comparison also substantiates the use of correlation energies of about 0.135 Ry, as these can be used to predict the magnetic moment correctly over the entire range of Fe concentration x .

V. SUMMARY AND CONCLUSION

The substitutional series of the quaternary Heusler compound $\text{Co}_2\text{Mn}_{1-x}\text{Fe}_x\text{Si}$ was synthesized and investigated both experimentally and theoretically.

The results found from the LDA+ U calculations for the magnetic moments $m(x)$ closely follow the Slater-Pauling curve. The shift of the minority gap with respect to the Fermi

energy, from the top of the minority valence band for Co_2MnSi to the bottom of the minority conduction band for Co_2FeSi , makes both systems rather unstable with respect to their electronic and magnetic properties. The calculated band structures suggest that the most stable compound in a half-metallic state will occur at an intermediate Fe concentration. These theoretical findings are supported by the experiments.

All samples of the substitutional series exhibit an $L2_1$ order that is independent of the Fe concentration x . The observed structural order-disorder phase transition from $L2_1 \leftrightarrow B2$ is nearly independent of x and occurs at about 1030 K. Mössbauer measurements show only a small paramagnetic contribution confirming the high degree of order over the whole substitutional series. In agreement with the expectation from the Slater-Pauling curve, the magnetic moment increases linearly with x from $5 \mu_B$ to $6 \mu_B$.

From both the experimental and computational results it is concluded that a compound with an intermediate Fe concentration would be best suited for spintronic applications.

Acknowledgments

The authors are grateful for the support by G. Schönhense and thank J. Thoenies and A. Lotz for help with the calculation of U_{eff} as well as V. Ksenofontov and S. Reimann for performing the Mössbauer experiments. Financial support by the DFG (projects TP1 and TP7 in research group FG 559) is gratefully acknowledged.

- [1] J. Kübler, A. R. Williams, and C. B. Sommers, Phys. Rev. B **28**, 1745 (1983).
- [2] R. A. d. Groot, F. M. Müller, P. G. v. Engen, and K. H. J. Buschow, Phys. Rev. Lett. **50**, 2024 (1983).
- [3] I. Galanakis, P. H. Dederichs, and N. Papanikolaou, Phys. Rev. B **66**, 174429 (2002).
- [4] S. Picozzi, A. Continenza, and A. J. Freeman, Phys. Rev. B **66**, 094421 (2002).
- [5] G. H. Fecher, H. C. Kandpal, S. Wurmehl, and C. Felser, J. Appl. Phys. **accepted** (cond-mat/0510210).
- [6] S. Picozzi, A. Continenza, and A. J. Freeman, Phys. Rev. B **69**, 094423 (2004).
- [7] S. Fuji, S. Sugimura, S. Ishida, and S. Asano, J. Phys.: Condens. Matter **2**, 8583 (1990).

[8] P. J. Brown, K.-U. Neumann, P. J. Webster, and K. R. A. Ziebeck, *J. Phys.: Condens. Matter* **12**, 1827 (2000).

[9] M. P. Raphael, B. Ravel, Q. Huang, M. A. Willard, S. F. Cheng, B. N. Das, R. M. Stroud, K. M. Bussmann, J. H. Claassen, and V. G. Harris, *Phys. Rev. B* **66**, 104429 (2002).

[10] U. Geiersbach, A. Bergmann, and K. Westerholt, *J. Magn. Magn. Mater.* **240**, 546 (2002).

[11] S. Kämmerer, S. Heitmann, D. Meyners, D. Sudfeld, A. Thomas, A. Hütten, and G. Reiss, *J. Appl. Phys.* **93**, 7945 (2003).

[12] L. J. Singh, Z. H. Barber, Y. Miyoshi, Y. Bugoslavsky, W. R. Branford, and L. F. Cohen, *Appl. Phys. Lett.* **84**, 2367 (2004).

[13] W. H. Wang, M. Przybylski, W. Kuch, L. I. Chelaru, J. Wang, F. Lu, J. Barthel, H. L. Meyerheim, and J. Kirschner, *Phys. Rev. B* **71**, 144416 (2005).

[14] W. H. Wang, M. Przybylskia, W. Kuch, L. I. Chelaru, J. Wang, Y. F. Lu, J. Barthel, and J. Kirschner, *J. Magn. Magn. Mat.* **286**, 336 (2005).

[15] J. Schmalhorst, S. Kammerer, M. Sacher, G. Reiss, A. Hütten, and A. Scholl, *Phys. Rev. B* **70**, 024426 (2004).

[16] J. Schmalhorst, S. Kammerer, G. Reiss, and A. Hütten, *Appl. Phys. Lett.* **86**, 052501 (2005).

[17] P. LeClair, H. J. M. Swagten, J. T. Kohlhepp, and W. J. M. de Jonge, *Appl. Phys. Lett.* **76**, 3783 (2000).

[18] S. Wurmehl, G. H. Fecher, H. C. Kandpal, V. Ksenofontov, C. Felser, H.-J. Lin, and J. Morais, *Phys. Rev. B* **72**, 184434 (2005).

[19] S. Wurmehl, G. H. Fecher, H. C. Kandpal, V. Ksenofontov, C. Felser, and H.-J. Lin, *Appl. Phys. Lett.* **88**, 032503 (2006).

[20] S. Wurmehl, G. H. Fecher, K. Kroth, F. Kronast, H. A. Dürr, Y. Takeda, Y. Saitoh, K. Kobayashi, H.-J. Lin, G. Schönhense, et al., *J. Phys. D: Appl. Phys.* **39**, 803 (2006).

[21] H. C. Kandpal, G. H. Fecher, and C. Felser, *Phys. Rev. B* accepted (cond-mat/0601671).

[22] Y. Miura, K. Nagao, and M. Shirai, *Phys. Rev. B* **69**, 144413 (2004).

[23] K. Kobayashi, R. Y. Umetsu, R. Kainuma, K. Ishida, T. Oyamada, A. Fujita, and K. Fukamichi, *Appl. Phys. Lett.* **85**, 4684 (2004).

[24] G. H. Fecher, H. C. Kandpal, S. Wurmehl, J. Morais, H.-J. Lin, H.-J. Elmers, G. Schönhense, and C. Felser, *J. Phys. Condens. Matter* **17**, 7237 (2005).

[25] P. Blaha, K. Schwarz, G. K. H. Madsen, D. Kvasnicka, and J. Luitz, *WIEN2k, An Augmented*

Plane Wave + Local Orbitals Program for Calculating Crystal Properties (Karlheinz Schwarz, Techn. Universitaet Wien, Wien, Austria, 2001).

- [26] J. P. Perdew, J. A. Chevary, S. H. Vosko, K. A. Jackson, M. R. Pederson, D. J. Singh, and C. Fiolhais, Phys. Rev. B **46**, 6671 (1992).
- [27] H. Ebert, in *Electronic Structure and Physical Properties of Solids. The Use of the LMTO Method*, edited by H. Dreysee (Springer-Verlag, Berlin, Heidelberg, 1999), vol. 535 of *Lecture Notes in Physics*, pp. 191 – 246.
- [28] V. I. Anisimov, F. Aryasetiawan, and A. I. Lichtenstein, J. Phys. Condens. Matter **9**, 767 (1997).
- [29] V. I. Anisimov and O. Gunnarson, Phys. Rev. B **43**, 7570 (1991).
- [30] G. K. H. Madsen and P. Novak, Europhys. Lett. **69**, 777 (2005).
- [31] V. I. Anisimov, J. Zaanen, and O. K. Andersen, Phys. Rev. B **44**, 943 (1991).
- [32] T. Bandyopadhyay and D. D. Sarma, Phys. Rev. B **39**, 3517 (1989).
- [33] D. Jung, H. J. Koo, and M. H. Whangbo, J. Molec. Struct. Theochem. **527**, 113 (2000).
- [34] G. E. Bacon and J. S. Plant, J. Phys. F: Met. Phys. **1**, 524 (1971).
- [35] V. Niculescu, T. J. Burch, K. Rai, and J. I. Budnick, J. Magn. Magn. Mater. **5**, 60 (1977).
- [36] V. Niculescu, J. I. Budnick, W. A. Hines, K. Rajt, S. Pickart, and S. Skalski, Phys. Rev. B **19**, 452 (1979).
- [37] K. Kobayashi, R. Y. Umetsu, A. Fujita, K. Oikawa, R. Kainuma, K. Fukamichi, and K. Ishida, J. All. Comp. **399**, 60 (2005).
- [38] P. J. Webster, J. Phys. Chem. Solids **32**, 1221 (1971).
- [39] M. Kallmayer, H. J. Elmers, B. Balke, S. Wurmehl, F. Emmerling, G. H. Fecher, and C. Felser, J. Phys. D: Appl. Phys. **39**, 786 (2006).
- [40] Note that 4a and 4b positions are equivalent; for clarity we assume that Si is always on 4b.
- [41] Note that the Mössbauer-data reported in Ref.[18] were taken at lower temperature (85K).